MCB
Journals.ASM.org

Insulin Stimulates Syntaxin4 SNARE Complex Assembly via a Novel Regulatory Mechanism

Dimitrios Kioumourtzoglou, Gwyn W. Gould, Nia J. Bryant*

Institute of Molecular, Cell and Systems Biology, College of Medical, Veterinary and Life Sciences, University of Glasgow, Glasgow, United Kingdom

Insulin stimulates glucose transport into fat and muscle cells by increasing the exocytic trafficking rate of the GLUT4 facilitative glucose transporter from intracellular stores to the plasma membrane. Delivery of GLUT4 to the plasma membrane is mediated by formation of functional SNARE complexes containing syntaxin4, SNAP23, and VAMP2. Here we have used an *in situ* proximity ligation assay to integrate these two observations by demonstrating for the first time that insulin stimulation causes an increase in syntaxin4-containing SNARE complex formation in adipocytes. Furthermore, we demonstrate that insulin brings about this increase in SNARE complex formation by mobilizing a pool of syntaxin4 held in an inactive state under basal conditions. Finally, we have identified phosphorylation of the regulatory protein Munc18c, a direct target of the insulin receptor, as a molecular switch to coordinate this process. Hence, this report provides molecular detail of how the cell alters membrane traffic in response to an external stimulus, in this case, insulin.

A major consequence of insulin binding its receptor on fat and muscle cells is a change in localization of the GLUT4 facilitative glucose transporter. In the absence of insulin, ~95% of the transporter is retained intracellularly. Activation of the insulin receptor tyrosine kinase culminates in a 10- to 20-fold increase in the amount of GLUT4 present at the cell surface, accounting for the increased rate of glucose transport into these cells (1). GLUT4 is sequestered away from the cell surface in the absence of insulin by continually cycling through two interrelated endosomal cycles (1). The first operates between the plasma membrane and early and recycling endosomes. This is a fast-trafficking loop that keeps steady-state levels of transporter at the cell surface low under basal conditions. GLUT4 is further sorted from this cycle into a more slowly operating loop between recycling endosomes, the *trans*-Golgi network, and a population of vesicles termed GSVs (GLUT4 storage vesicles). It is from GSVs that GLUT4 is mobilized to the cell surface in response to insulin (1).

Like all eukaryotic membrane trafficking events, insulin-regulated trafficking of GLUT4 is mediated by formation of specific SNARE complexes. Cell surface delivery of GLUT4 is mediated by a SNARE complex containing the plasma membrane-localized syntaxin4 (Sx4) and SNAP23 t-SNAREs and the VAMP2 v-SNARE (2). SNARE complex formation contributes to specificity of membrane traffic and also provides energy for bilayer fusion (3). Thus, regulating SNARE complex assembly allows the cell to regulate membrane traffic, but whether insulin stimulates SNARE complex formation remains unknown. Sec1/Munc18 (SM) proteins are key regulators of membrane traffic exerting their effect through their cognate SNARE proteins, but their precise mode of action is not understood (3). The Munc18c SM protein binds to Sx4 and is required for insulin-regulated delivery of GLUT4 to the surface of fat and muscle cells (2). Intriguingly, Munc18c is phosphorylated in response to insulin, with Tyr521 being a direct target of the activated insulin receptor (4–6). Evidence for functional consequences of this phosphorylation comes from the observation that, in contrast to phosphomimetic mutation, phosphoresistant mutation of this site removes the ability of Munc18c to rescue the defective insulin-stimulated GLUT4 translocation seen in Munc18c knockdown adipocytes (4–6). These observations suggest that phosphorylation of Munc18c could provide a direct link between activation of the insulin receptor's tyrosine kinase activity and delivery of GLUT4 to the cell surface in response to insulin and make it tempting to hypothesize that insulin increases GLUT4 delivery to the cell surface by regulating assembly of the Sx4-containing SNARE complex.

Here we have used an *in situ* proximity ligation assay (PLA) to test this hypothesis directly. By observing changes in associations between Sx4, SNAP23, VAMP2, and Munc18c in response to insulin in adipocytes, we show that there is an increase in the number of Sx4-containing SNARE complexes following insulin stimulation. In addition, we also resolve two functionally distinct pools of Sx4 and suggest that one facilitates basal recycling of GLUT4 through the plasma membrane in the absence of insulin and that the second is held in an inactive state until it is mobilized in response to insulin to accommodate the bolus delivery of GLUT4 to the cell surface observed under these conditions. Finally, we identify a role for phosphorylation of the Munc18c SNARE regulator by the tyrosine kinase insulin receptor in mobilizing the inactive pool of Sx4. Collectively, these data provide novel insight into the molecular mechanisms by which insulin increases the rate of glucose transport into adipocytes by demonstrating that insulin drives formation of SNARE complexes that deliver GLUT4 to the cell surface and that this effect is mediated through phosphorylation of Munc18c.

Received 10 September 2013 **Returned for modification** 3 October 2013
Accepted 7 January 2014

Published ahead of print 27 January 2014

Address correspondence to Nia J. Bryant, nia.bryant@york.ac.uk, or Gwyn W. Gould, gwyn.gould@glasgow.ac.uk.

* Present address: Nia J. Bryant, Department of Biology, University of York, Heslington, York, United Kingdom.

Supplemental material for this article may be found at http://dx.doi.org/10.1128/MCB.01203-13.

Copyright © 2014, American Society for Microbiology. All Rights Reserved.

doi:10.1128/MCB.01203-13

TABLE 1 Proteins produced in this study

Protein	Description	Reference or source
GST-Sx4	Residues 1–273 of Sx4 tagged N terminally with GST; thrombin cleavable	7
Sx4-GST	Residues 1–273 of Sx4 tagged C terminally with GST	7
$_{\Delta N36}$Sx4-GST	Residues 37–273 of Sx4 tagged C terminally with GST	7
$_{open}$Sx4-GST	Residues 1–273 of Sx4 tagged harboring two point mutations ($L_{173}/E_{174}A$) tagged C terminally with GST	7
GST-$_{\Delta Habc}$Sx4	Residues 200–273 of Sx4 tagged N terminally with GST; thrombin cleavable	This study
GST-SNAP23	Residues 1–211 of SNAP23 tagged N terminally with GST; thrombin cleavable	8
His-SNAP23	Residues 1–211 of SNAP23 tagged N terminally with His_6; thrombin cleavable	This study
GST-VAMP2	Residues 1–91 of VAMP2 tagged N terminally with GST; thrombin cleavable	This study
VAMP2-PrA	Residues 1–91 of VAMP2 tagged C terminally with PrA	This study
GST-$_{\Delta N30}$VAMP2	Residues 31–91 of VAMP2 tagged N terminally with GST; thrombin cleavable	9
His-Munc18c	N-terminally His_6-tagged Munc18c (residues 1–592)	9
His-Munc18c$_{Y521E}$	N-terminally His_6-tagged Munc18c (residues 1–592) harboring a $Y_{521}E$ mutation	4
Snc2-PrA	Residues 1–88 of Snc2 C terminally tagged with PrA	10

MATERIALS AND METHODS

Antibodies. The antibodies used were anti-Munc18c (Abcam catalogue no. ab26331; Novus Biologicals catalogue no. H00006814-B010), anti-SNAP23 (Santa Cruz Biotechnology Inc. catalogue no. sc-101303, Synaptic Systems catalogue no. 111203), anti-syntaxin4 (BD Transduction Laboratories catalogue no. 610439, Abcam catalogue no. ab77037; Synaptic Systems catalogue no. 110042), anti-VAMP2 (Abcam catalogue no. ab18014; Synaptic Systems catalogue no. 104 211), and anti-His6 (Sigma catalogue no. H1029).

Recombinant proteins. Recombinant proteins described in Table 1 were expressed heterologously in *Escherichia coli* [BL21(DE3); Invitrogen]. Proteins were purified using Ni^{2+}-nitrotriacetic acid-agarose (Qiagen) or IgG- or glutathione-Sepharose (GE Healthcare). Resins were added such that the tagged protein was in excess of the available binding sites to saturate the resin.

Plasmids made during the course of this study. Plasmids to produce the following proteins were made as follows. The glutathione *S*-transferase (GST)–$_{\Delta Habc}$Sx4 (and $_{\Delta Habc}$Sx4, which is produced by removal of the GST tag by cleavage with thrombin) sequence encoding the SNARE domain of Sx4 from pETDuet:Sx4-GST (7) was amplified by PCR with the addition of BamHI (5′) and EcoRI (3′) restriction sites and subcloned into pGEX-4T-1. The His-SNAP23 sequence encoding SNAP23 from 3T3-L1 adipocyte cDNA was amplified by PCR with the addition of BamHI (5′) and HindIII (3′) sites and subcloned into pQE30. The VAMP2-PrA sequence encoding the cytosolic domain of rat VAMP2 was amplified by PCR with the addition of NdeI (5′) and XhoI (3′) restriction sites, using C-terminally as a template a full-length VAMP2 construct (9), and subcloned into pCOG022 (10). The GST-VAMP2 sequence encoding the cytosolic domain of rat VAMP2 from the construct described above was amplified by PCR with the addition of BamHI (5′) and EcoRI (3′) restriction sites and subcloned into pGEX-4T-1.

PLA. 3T3-L1 adipocytes were grown on Labtech 8-chamber slides. Following insulin stimulation where indicated, cells were washed 3 times with phosphate-buffered saline (PBS) (85 mM NaCl, 1.7 mM KCl, 5 mM Na_2HPO_4, 0.9 mM KH_2PO_4, pH 7.4) prior to fixation (30 min in 3% [wt/vol] paraformaldehyde). Two washes with GLY (20 mM glycine–PBS) followed before cells were blocked and permeabilized in BSA-GLY-SAP solution (0.1% [wt/vol] saponin, 2% [wt/vol] bovine serum albumin [BSA], GLY) for 30 min. Primary antibody incubations were performed in BSA-GLY-SAP solution overnight at 37°C in a humidity incubator, after which PLA was performed according to the instructions of the manufacturer (Duolink In Situ PLA kit; Olink Bioscience). Signals were visualized using a Zeiss LSM Pascal Exciter fluorescence system with a 63× oil immersion objective. For quantification, signals in 30 to 100 cell images were counted using Blobfinder version 3.2 (11). The following parameters were used throughout the analysis: blob threshold, 120 (arbitrary units); minimum nucleus size, 100 pixels; cytoplasm size, 200 pixels; blob size, 3 by 3 pixels. The Mann-Whitney U test was performed for statistical analysis of the PLA results (SPSS software). Box plots display median values of signal per cell from 30 to 100 cells. Figures and plots are representative of the results of 3 independent experiments.

RESULTS

Insulin stimulates formation of syntaxin4/SNAP23/VAMP2/Munc18c-containing SNARE complexes. The issue of whether insulin regulates assembly of Sx4-containing SNARE complexes as a mechanism to regulate GLUT4 exocytosis has been problematic to address. We and others have previously performed coimmunoprecipitation experiments to ask whether insulin stimulation of adipocytes leads to changes in associations between Sx4, SNAP23, VAMP2, and Munc18c but have been unable to exclude the possibility that changes in interactions occur post-cell lysis. Microscopy-based approaches using fluorescence resonance energy transfer (FRET) or bipartite fluorescent proteins to follow changes in associations in response to insulin circumvent the need to lyse cells but require the addition of tags to the proteins of interest. Addition of tags to SNARE proteins can alter their function and interaction profile, making interpretation of data obtained using such techniques unreliable (7). To overcome these problems, we have used a microscopy-based proximity ligation assay (PLA) to follow changes in associations between endogenous Sx4, SNAP23, VAMP2, and Munc18c in 3T3-L1 adipocytes in response to insulin. This technique relies on antibodies against the two proteins of interest being raised in separate species. These can then be detected using species-specific secondary antibodies to which short oligonucleotides of different defined sequences are covalently attached. A PLA signal is obtained only when the oligonucleotides coupled to the secondary antibodies are sufficiently close to allow hybridization and subsequent enzymatic ligation of added connector oligonucleotides; this, in turn, is determined by the proximity of the two antigens of interest. Detection relies on amplification from the ligated template through rolling PCR, followed by hybridization of a fluorescent probe (12, 13). Associations between the two antigens can be visualized by confocal microscopy, with the number of fluorescent spots detected being directly proportional to the number of associations between the two proteins (14).

Figure 1 presents visualizations of pairwise associations be-

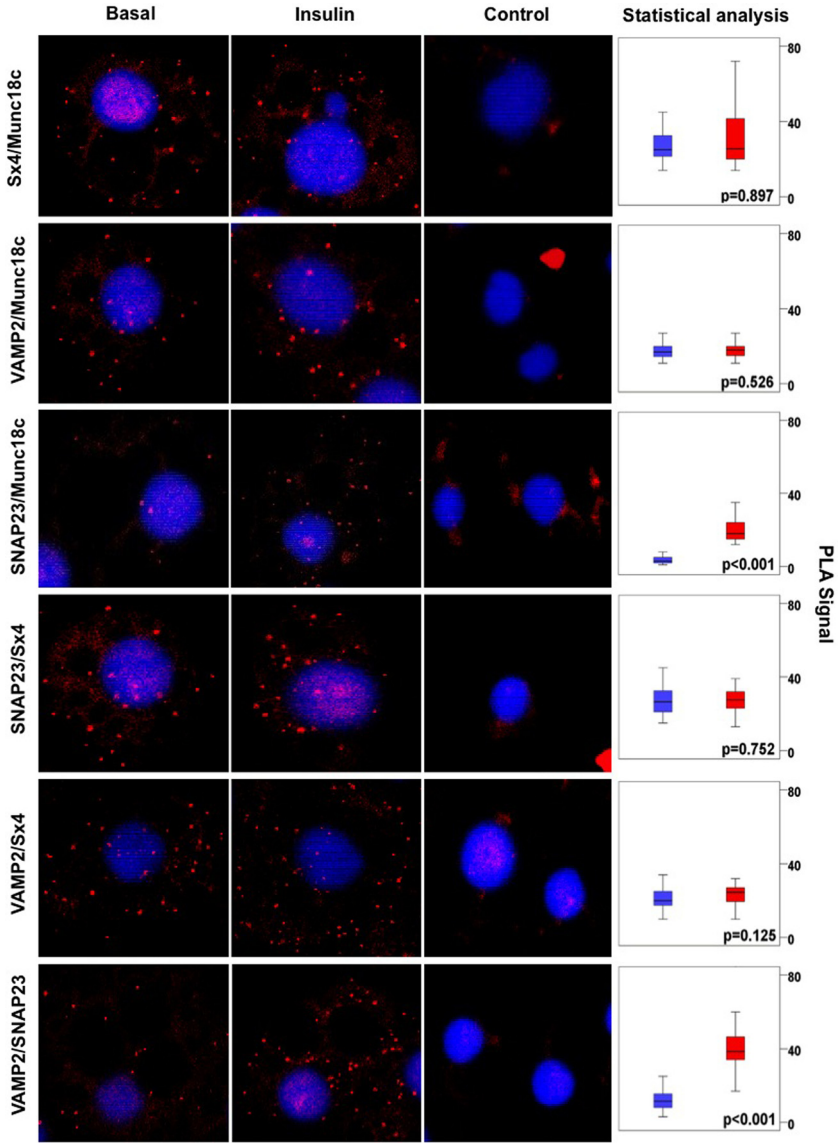

FIG 1 Pairwise associations between syntaxin4, SNAP23, VAMP2, and Munc18c in 3T3-L1 adipocytes in the presence and absence of insulin stimulation. PLA results of pairwise associations between Sx4, SNAP23, VAMP2, and Munc18c in 3T3-L1 adipocytes treated with 100 nM insulin for 5 min or not treated (basal) are shown in red (blue = DAPI [4′,6-diamidino-2-phenylindole]). Controls omitting the first listed primary antibody are shown for each pairwise combination. Statistical analyses of PLA results were performed using Blobfinder and SPSS software. Box plots represent median numbers of signals per cell from 30 to 100 cells per experiment (*y* axis; blue = basal, red = insulin). Images are representative of the results of 3 independent experiments. For all control experiments, the PLA signal value was <1 per cell. Signal obtained in the presence of both primary antibodies was found to be significantly greater than that obtained in controls for all combinations shown ($P < 0.001$).

tween Sx4, SNAP23, VAMP2, and Munc18c using PLA in 3T3-L1 adipocytes in the absence and presence of insulin. Note that a positive signal by PLA does not necessarily indicate a direct interaction between the two proteins being detected. The length of the oligonucleotides coupled to the secondary antibodies requires that the antigens are within 15 nm of each other. This is within the size of an assembled SNARE complex (15), and it is likely that this structure represents the source of the positive signal between pairs of proteins that do not interact directly with each other (i.e., SNAP23/VAMP2 and SNAP23/Munc18c) (see Fig. S1-2 in the supplemental material).

Statistical analyses of quantitation of images of ≥30 cells from each of three independent experiments for the 6 possible pairwise combinations between Sx4, SNAP23, VAMP2, and Munc18c under both basal and insulin-stimulated conditions (Fig. 1) revealed insulin-dependent changes in only two of these associations, namely, those between SNAP23 and VAMP2 and between SNAP23 and Munc18c, both of which increase in response to insulin (control experiments indicated that insulin stimulation of adipocytes does not mask or reveal any epitopes recognized by the antibodies used here [see Fig. S1-1 in the supplemental material]; it is also important that the expression levels of the proteins followed are similar to each other in 3T3-L1 adipocytes [16] and are not affected by acute insulin stimulation [5, 17–19]).

Although SNAP23 does not bind directly to either VAMP2 or Munc18c (see Fig. S1-2 in the supplemental material), Munc18c binds the assembled Sx4/SNAP23/VAMP2 complex (20), which contains both SNAP23 and VAMP2 in close enough proximity to generate a positive PLA signal with the oligonucleotides used. Thus, the concomitant increase in the numbers of associations of SNAP23 with VAMP2 and Munc18c in response to insulin support a model in which insulin stimulation increases the number of assembled Sx4/SNAP23/VAMP2 SNARE complexes and in which these have Munc18c associated with them.

There are several mechanistic possibilities that could explain how insulin stimulation leads to the increased PLA associations between SNAP23 and Munc18c and between SNAP23 and VAMP2 presented in Fig. 1. The simplest is that insulin action results in ternary complex formation from monomeric Sx4, SNAP23, and VAMP2 and that Munc18c binds to these assembled complexes. An alternative possibility is that the t-SNARE complex of Sx4/SNAP23 is preformed under basal conditions, either with or without Munc18c bound. Insulin could then drive association of this with VAMP2 (and recruit Munc18c in the case of the SM protein not being prebound to the t-SNARE). These possibilities predict different changes in pairwise associations between Sx4, SNAP23, VAMP2, and Munc18c in response to insulin. Were insulin to stimulate the coming together of all 4 proteins from monomeric pools, increases in all pairwise associations would occur. This model is not consistent with the data presented in Fig. 1, as no increase in associations of Sx4 with any of SNAP23, VAMP2, and Munc18c are seen. This indicates that Sx4 is associated with all of these proteins prior to insulin stimulation as well as after. It is clear that they are not all in complex together since we saw an increase in associations between VAMP2 and SNAP23 in response to insulin (Fig. 1), indicating that at least two distinct pools of Sx4 existed under basal conditions: one in complex with SNAP23 and one in complex with VAMP2. In support of this, Sx4/SNAP23 binary t-SNARE complex formation is not affected by insulin stimulation of adipocytes, and t-SNARE complex formation precedes SNARE complex formation in other systems (18). It has also previously been shown that Sx4 binds directly to VAMP2 in the absence of SNAP23 (21), and a similar interaction between VAMP2 and neuronal syntaxin1A has been characterized (22, 23). The presence of these distinct pools of Sx4 in basal cells would explain the increase in associations observed between SNAP23 and VAMP2 in the absence of concomitant increases in associations of Sx4 with VAMP2 and SNAP23 upon insulin-stimulated ternary complex formation. Similarly, no changes in the number of associations between Munc18c and Sx4 were observed (Fig. 1), indicating that these two proteins are in association under basal conditions. This, taken in conjunction with the observed increase in the number associations between Munc18c and SNAP23 in the absence of any change in the number of associations between Munc18c and VAMP2, indicates that Munc18c is associated with the pool of Sx4 in association with VAMP2 and not with the Sx4-SNAP23 pool. In summary, the data presented in Fig. 1 indicate that there are two pools of Sx4 in adipocytes under basal conditions, one in complex with SNAP23 and one in complex with VAMP2, and that Munc18c is associated with the latter but not the former.

Interaction between the cytosolic domains of VAMP2 and syntaxin4 is inhibitory to SNARE complex formation. As discussed above, as well as participating in the ternary SNARE complex, Sx4 forms binary complexes with both SNAP23 and VAMP2 (18, 20, 21). Figure 2 shows that the cytosolic domains of Sx4 and VAMP2 bind directly to each other in a specific manner. A protein A (PrA) fusion harboring the cytosolic domain of VAMP2 (residues 1 to 91) bound to IgG-Sepharose pulls down the cytosolic domain of Sx4 (residues 1 to 211) in a time-dependent manner (Fig. 2A). Similarly, a GST fusion containing the cytosolic domain of Sx4 pulls down purified VAMP2-PrA (Fig. 2B). Importantly, the specificity of the Sx4/VAMP2 interaction is demonstrated by the observation that Sx4-GST does not bind a PrA fusion protein carrying the cytosolic domain of the noncognate R(v)-SNARE Snc2 (Fig. 2B). The cytosolic portion of syntaxins comprises 3 separate domains (24), each of which facilitates protein-protein interactions: the N peptide, the Habc domain, and the SNARE domain (24). To characterize further the interaction between VAMP2 and Sx4, we investigated the ability of mutant versions of Sx4-GST to pull down the cytosolic domain of VAMP2. Figure 2 shows that removing the N peptide of Sx4 (in $_{\Delta_{N36}}$Sx4-GST) had no effect on its ability to bind the cytosolic domain of VAMP2 (Fig. 2C and F). In contrast, introduction of mutations shown to "lock" Sx4 in an open conformation ($_{open}$Sx4-GST) and removal of the Habc domain of Sx4 ($_{\Delta_{Habc}}$Sx4-GST) (7) both enhance the rate at which VAMP2 is pulled down (Fig. 2D to F) due to the increased availability of the SNARE domain shown by their increased rate of entry into SNARE complexes (see Fig. S4A and B in the supplemental material) as observed for other syntaxins (25–27). These data demonstrate that the direct, specific interaction between the cytosolic domains of Sx4 and VAMP2 is mediated by Sx4's SNARE motif.

As reported for other 4-helical SNARE complexes, the SNARE motifs of Sx4, VAMP2, and SNAP23 form a highly stable complex that is SDS resistant (8, 28). This characteristic feature forms the basis of a useful assay to follow assembly of purified recombinant proteins into SNARE complexes *in vitro* (Fig. 3). Incubation of the cytosolic domain of Sx4 with His-tagged SNAP23 and GST-tagged VAMP2 resulted in formation of an SDS-resistant complex of ~100 kDa (Fig. 3, lanes 7 to 9), representing the combined molecular masses of the three proteins. Formation of this complex required all three proteins, indicated by the observation that the complex did not form when GST was included in place of GST-VAMP (Fig. 3, lanes 10 to 12); similarly, the complex was not formed when either Sx4 or SNAP23 was omitted from the reaction (see Fig. S3-1 in the supplemental material). Previous studies have shown that preformation of t-SNARE complexes enhances the rate of SNARE complex assembly (26, 29). Consistent with this, preincubation of Sx4 with SNAP23 increased the rate of SNARE complex formation using our assay (Fig. 3; compare lanes 4 to 6 and lanes 7 to 9). In contrast, preincubation of Sx4 with VAMP2 was inhibitory to the same reaction (lanes 1 to 3) (see also Fig. S3-2 in the supplemental material). These data indicate that, in contrast to the Sx4/SNAP23 interaction, the Sx4/VAMP2 binary interaction is inhibitory to SNARE complex formation.

Munc18c stimulates SNARE complex assembly by alleviating the inhibition of the syntaxin4/VAMP2 binary interaction. Despite its clear importance, the role of Munc18c in insulin-stimulated delivery of GLUT4 to the plasma membrane is poorly understood. We have previously shown that Munc18c has an inhibitory effect on Sx4/SNAP23/VAMP2-mediated membrane fusion (9) whereas other SM proteins stimulate the fusion events that they regulate (29, 30). The data presented in Fig. 4A and B show that the same recombinant Munc18c inhibited formation of SDS-

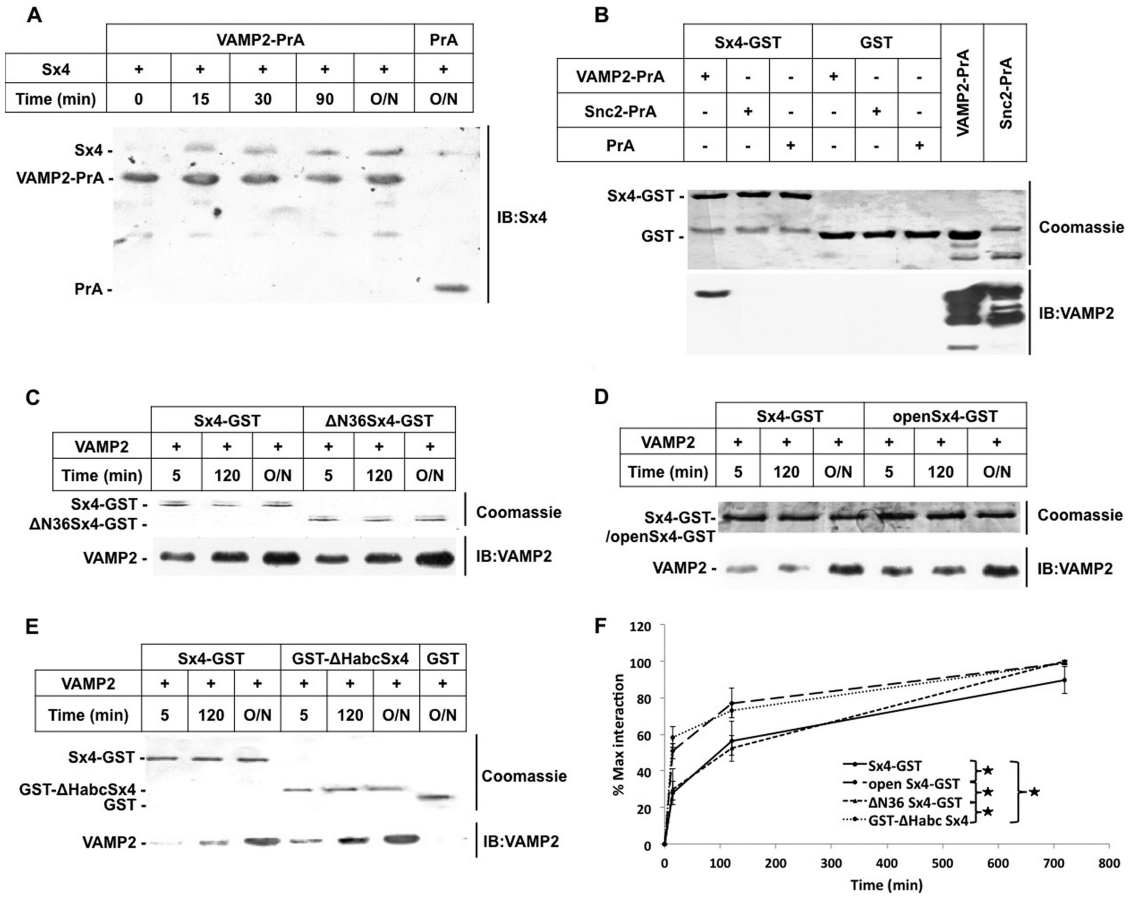

FIG 2 Direct interaction between the cytosolic domain of VAMP2 and the SNARE motif of syntaxin4. (A) A 10-μg amount of VAMP2-PrA or PrA bound to IgG-Sepharose (10-μl bed volume) was incubated with a 10× molar excess of the cytosolic domain of Sx4 (cleaved from GST-Sx4) in 1 ml PBS at 4°C for the indicated times. Beads were washed with PBS prior to resuspension in Laemmli sample buffer (LSB) and heating to 95°C for 5 min. Eluted proteins were subjected to SDS-PAGE using a 15% separating gel and visualized by immunoblot (IB) analysis using anti-Sx4 antibody (which recognizes both Sx4 and PrA moieties). (B) A 30-μg amount of Sx4-GST or GST bound to glutathione-Sepharose beads (10-μl bed volume) was incubated with a 10× molar excess of VAMP2-PrA, Snc2-PrA, or PrA in 1 ml PBS at 4°C for 2 h. Beads were washed using PBS prior to resuspension in LSB and heating to 95°C for 5 min. Eluted proteins were subjected to SDS-PAGE using a 15% separating gel and visualized by Coomassie blue staining and immunoblot analysis (which recognizes all PrA moieties). VAMP2-PrA and Snc2-PrA were loaded for reference. (C to E) A 10- to 30-μg amount of Sx4-GST, $_{\Delta N36}$Sx4-GST, $_{open}$Sx4-GST, GST-$_{\Delta Habc}$Sx4, or GST bound to glutathione-Sepharose beads (10-μl bed volume) was incubated with a 10× molar excess of the cytosolic domain of VAMP2 (cleaved from GST-VAMP2) in 1 ml PBS at 4°C for the indicated times. Beads were then washed using PBS prior to resuspension in LSB and heating to 95°C for 5 min. Eluted proteins were subjected to SDS-PAGE using a 15% separating gel and subjected to Coomassie blue staining to visualize the input GST proteins and to immunoblot analysis using anti-VAMP2 antibody to estimate the amount of VAMP2 bound. (F) Comparison of the abilities of Sx4-GST and mutants thereof to bind the cytosolic portion of VAMP2 (C to E). The proportion of VAMP2 pulled down by the different versions of Sx4-GST (expressed as a percentage of maximum binding) is plotted as a function of time. Error bars represent the standard deviations of the variable percentage (VAMP2) of the maximum signal intensity values determined in 3 independent experiments (data, expressed as the area under the curve, were statistically analyzed in pairs using a two-tailed *t* test; stars indicate $P < 0.05$).

resistant Sx4/SNAP23/VAMP2 complexes *in vitro*. For these experiments, a variation on the SNARE complex assembly assay was used. In this case, Sx4-GST bound to glutathione-Sepharose was preincubated with His-Munc18c or was not preincubated prior to the addition of SNAP23 and VAMP2. SNARE complexes bound to the beads were identified as high-molecular-mass immunoreactive bands whose time-dependent formation required the presence of Sx4, SNAP23, and VAMP2 (see Fig. S3-1 in the supplemental material).

Munc18c is a direct target of the insulin receptor, becoming phosphorylated on Tyr_{521} (4–6). Munc18c needs to be phosphorylated to perform its essential function in insulin-stimulated translocation of GLUT4 since phosphomimetic Munc18c ($Y_{521}E$) rescues defective insulin-regulated GLUT4 traffic in Munc18c knockdown adipocytes, whereas phosphoresistant versions do not (5). In contrast to wild-type Munc18c, which is inhibitory to the rate of Sx4-SNARE complex formation, *in vitro* introduction of the phosphomimetic $Y_{521}E$ mutation into this construct resulted in a protein that then stimulated SNARE complex formation (Fig. 4C and D).

The PLA data presented in Fig. 1 led us to hypothesize that there are two separate pools of Sx4 in adipocytes under basal conditions: one in association with SNAP23 and the other in association with VAMP2 and Munc18c. Our finding that, in contrast to the Sx4/SNAP23 binary interaction, binding of Sx4 to VAMP2 is inhibitory to SNARE complex formation raises the possibility that these two pools serve distinct functions. One possibility is that Sx4 in complex with SNAP23 facilitates the basal level of GLUT4 cy-

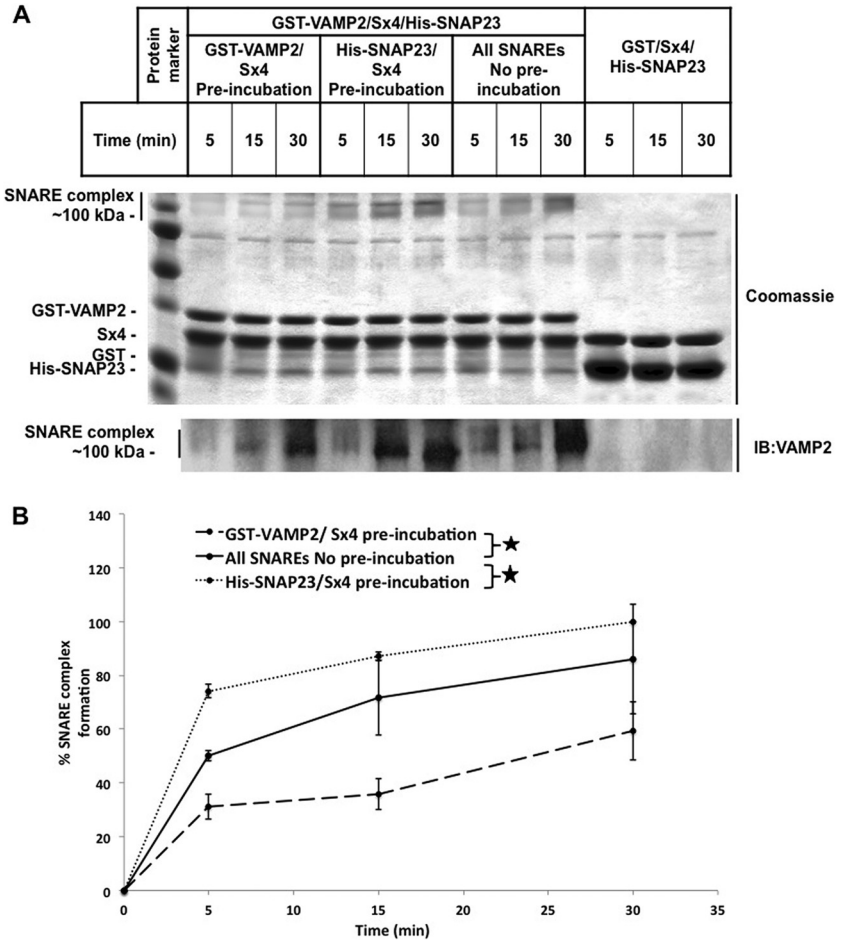

FIG 3 *In vitro* SNARE complex formation. (A) A 100- to 500-μg amount of the purified cytosolic domain of Sx4 (cleaved from GST-Sx4) was incubated in a 0.5-ml volume of PBS with GST-VAMP2 (lanes 1 to 3) or His-SNAP23 (lanes 4 to 6) or in PBS alone (lanes 7 to 12) for 2 h at 4°C. A 100- to 500-μg amount of the following proteins was then added in a final volume of 1 ml PBS containing 10 μg BSA: lanes 1 to 3, His-SNAP23; lanes 4 to 6, GST-VAMP2; lanes 7 to 9, His-SNAP23 and GST-VAMP2; lanes 10 to 12, His-SNAP23 and GST alone. Reaction mixtures were incubated at 37°C with mixing, and samples (100 μl) were taken after 5, 15, and 30 min as indicated. Following addition of LSB, samples were heated to 95°C for 10 min prior to SDS-PAGE using a 15% separating gel and Coomassie staining (upper panel) and immunoblot analysis using anti-VAMP2 antibody (lower panel). The protein marker included is Bio-Rad Precision Plus protein standards; the bands are, from the top, 100, 75, 50, 37, 25, and 20 kDa. (B) Quantification of SNARE complex formation data from panel A plotted as percentage of maximum complex formation against time. Error bars represent standard deviations of the variable percentage (SNARE complex) of the maximum signal intensity values from 3 independent experiments (data, expressed as the area under the curve, were statistically analyzed in pairs using a two-tailed *t* test; stars indicate $P < 0.05$).

cling through the cell surface observed in the absence of insulin whereas that in association with VAMP2/Munc18c provides a reservoir of Sx4 to be mobilized upon insulin stimulation to accommodate the rapid increase in GLUT4 delivery to the plasma membrane seen under these conditions. With this model in mind, we investigated the role of Munc18c in SNARE complex formation from Sx4 held in complex with VAMP2. The data presented in Fig. 4E and F show that phosphomimetic Y521E Munc18c alleviated the inhibitory effect of the Sx4/VAMP2 interaction whereas the wild-type SM protein did not.

DISCUSSION

The notion that cells can employ the regulation of SNARE complex formation as a means to control membrane traffic is attractive. It has long been postulated that in cells such as adipocytes, where acute insulin challenge promotes delivery of GLUT4-containing vesicles to the cell surface, insulin drives an increase in SNARE complex formation, but this important hypothesis lacks clear supporting evidence. Here, by following changes in pairwise associations between Sx4, SNAP23, VAMP2, and Munc18c in adipocytes, we observed insulin-stimulated changes that are consistent with insulin bringing about an increase in the number of assembled SNARE complexes. Analyses of the observed insulin-dependent changes also suggest the presence of two distinct pools of Sx4 in adipocytes under basal conditions: one in association with SNAP23 and the other in association with VAMP2 and Munc18c. Our biochemical data demonstrate that, in contrast to the Sx4/SNAP23 binary t-SNARE interaction which enhances SNARE complex formation, interaction between the cytosolic domains of Sx4 and VAMP2 is inhibitory to SNARE complex formation. We propose that these two distinct pools of Sx4 are also functionally distinct. In our model, the pool of Sx4 in complex with SNAP23 facilitates the level of GLUT4 cycling through the cell surface observed in the absence of insulin to achieve its steady-

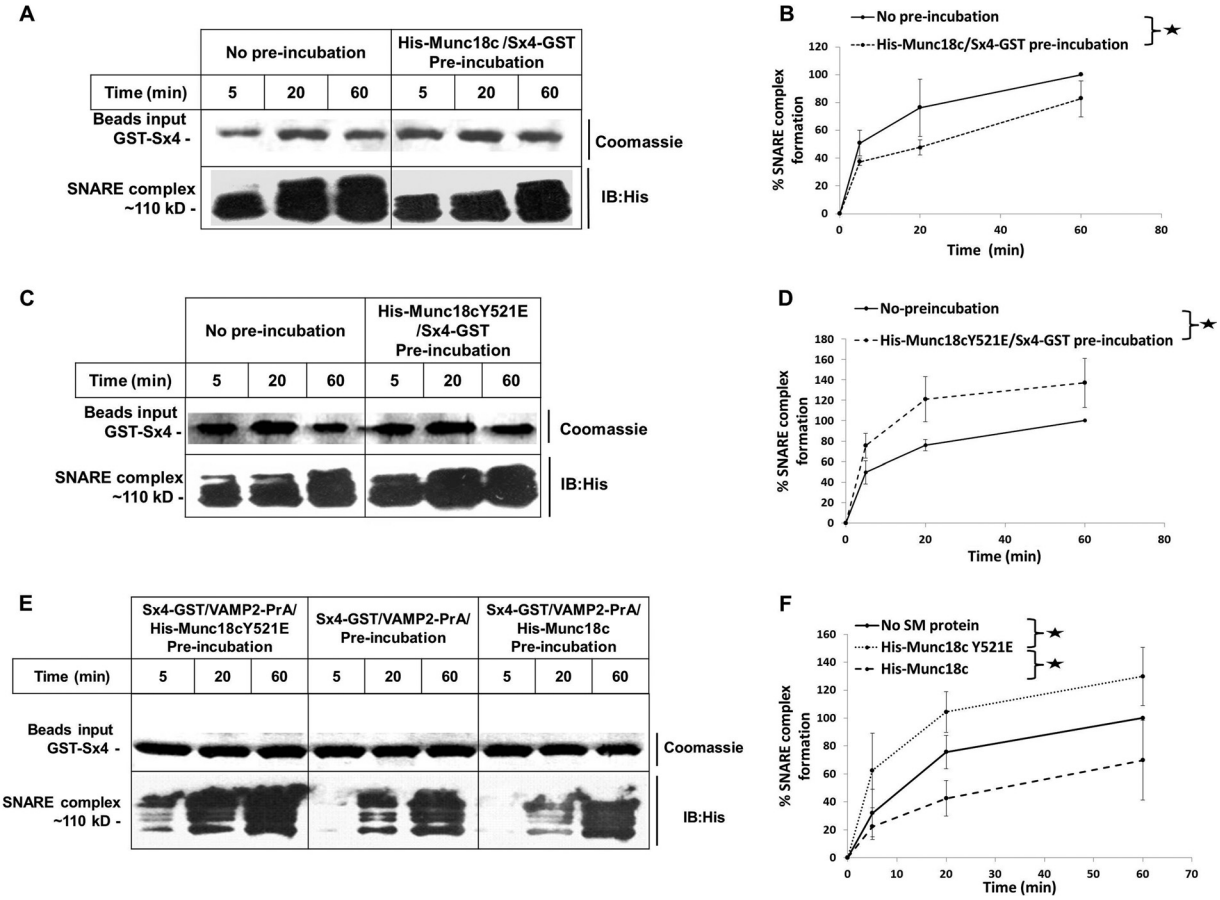

FIG 4 Effect of Munc18c on syntaxin4/SNAP23/VAMP2 SNARE complex formation. A 30- to 50-μg amount of Sx4-GST bound to glutathione-Sepharose (10-μl bed volume) was preincubated for 2 h at 4°C in a 1-ml volume with a 10× molar excess of His-Munc18c (A) or His-Munc18c$_{Y521E}$ (C) or PBS alone (no preincubation) prior to washing with PBS and resuspension in 1 ml PBS containing His-SNAP23 and VAMP2-PrA each in 10× molar excess. (E) Alternatively, Sx4-GST was preincubated in 1 ml PBS containing a 10× molar excess of VAMP2-PrA and His-Munc18c, Munc18c$_{Y521E}$, or no Munc18c for 2 h at 4°C prior to addition of a 10× molar excess His-SNAP23. In all cases, reaction mixtures were incubated at 4°C for the indicated times and beads were washed extensively using PBS prior to the addition of 50 μl 2× LSB and heating to 95°C for 5 min. Samples were subjected to SDS-PAGE using a 15% separating gel and visualized by Coomassie blue staining (upper panels [to control for equal input levels of Sx4-GST]) or immunoblot analysis using anti-His6 antibody (lower panel). Immunoreactivity at ~110 kDa corresponds to an SDS-resistant ternary complex containing Sx4-GST/His-SNAP23/VAMP-PrA (see Fig. S3-1 in the supplemental material). Data presented in panels A, C, and E are quantified in panels B, D, and F, respectively, with the proportion of SNARE complex formed expressed as a percentage of the maximum amount detected in the "No-preincubation" sample (B and D) or the no-SM (Sx4-GST/VAMP2-PrA-alone preincubation) sample (F), plotted as a function of time. Error bars represent standard deviations of the variable percentage (SNARE complex) of the maximum signal intensity values from 3 independent experiments (data, expressed as the area under the curve, were statistically analyzed in pairs using a two-tailed *t* test; stars indicate $P < 0.05$).

state intracellular sequestration. The pool of Sx4 in association with VAMP2 and Munc18c could provide a reservoir of the syntaxin ready to be mobilized upon insulin stimulation when a bolus of GLUT4 delivery to the plasma membrane is required.

This model predicts that VAMP2/GLUT4-containing vesicles docked with Sx4 at the cell surface fuse with the plasma membrane upon insulin stimulation, consistent with studies using total internal reflection fluorescence (TIRF) microscopy which demonstrated that the majority of GLUT4 is within 100 nm of the cell surface (31) (although in 3T3-L1 adipocytes which lack a single large lipid droplet, GLUT4 is found deeper within the cell [32], it is still clear that a key action of insulin in fusion of GSVs occurs at the plasma membrane [33]). Future studies combining PLA and TIRF microscopy might be able to identify this more precisely. We previously characterized a direct interaction between VAMP2 and Munc18c and showed that this can be disrupted by Sx4 (9). It is tempting to speculate that interaction of Munc18c with VAMP2 serves to carry GLUT4-containing vesicles to Sx4 present on the plasma membrane. Displacement of Munc18c from VAMP2 by Sx4 might then allow formation of Sx4/VAMP2 binary complexes to serve as a reservoir of Sx4, held in an inactive state through interaction with VAMP2 and ready to be mobilized by insulin. In this scenario, Munc18c would be associated with the VAMP2/Sx4 complex through interaction with Sx4.

Munc18c is a direct target of the insulin receptor, becoming phosphorylated on Tyr$_{521}$ (4–6). A phosphomimetic mutant (Y$_{521}$E) rescues defective insulin-regulated GLUT4 traffic in Munc18c knockdown adipocytes, whereas phosphoresistant versions do not (5). These data indicate that Munc18c needs to be phosphorylated to perform its essential function in insulin-stimulated translocation of GLUT4. Phosphomimetic mutation of Munc18c abrogates direct interaction with syntaxin4 (4). This is

not reflected in our PLA data due to a concomitant increase in the number of assembled SNARE complexes to which Munc18c binds (Fig. 1). Immunoprecipitation of Munc18c following peroxyvanadate treatment of adipocytes indicated reduced association with syntaxin4 (5). One possibility for the apparent discrepancy between our study and those data is that binding of Munc18c to Sx4 (binary interaction) is of greater affinity than that to the assembled SNARE complex and that the latter is disrupted during the cell lysis/immunoprecipitation procedure.

We have previously shown that wild-type (His_6-tagged) Munc18c is inhibitory to Sx4/SNAP23/VAMP2 complex-mediated liposome fusion (9). Consistent with that, we now show that the same wild-type Munc18c construct is inhibitory to Sx4-SNARE complex formation *in vitro*. Introduction of the phosphomimetic $Y_{521}E$ mutation into this construct results in a protein that now stimulates SNARE complex formation. Intriguing molecular insight into how this might be achieved is provided by our finding that phosphomimetic Munc18c alleviates the inhibitory effect of the VAMP2/Sx4 binary interaction on SNARE complex formation whereas wild-type Munc18c does not. These data identify Munc18c as a molecular switch whose phosphorylation in response to insulin drives Sx4-SNARE complex formation and thus facilitates delivery of GLUT4 to the cell surface.

The simplest model for stimulation of SNARE complex assembly and membrane fusion by SM proteins involves switching the syntaxin from a closed to an open conformation (25, 34). Consistent with this, phosphomimetic Munc18c does not increase the rate at which the open mutant of Sx4 forms SNARE complexes (see Fig. S4 in the supplemental material); similarly, no effect on the ability of Sx4 lacking the N peptide to form SNARE complexes is seen, suggesting that this region is required for the conformational switch. It is important to determine how the negative effect of wild-type Munc18c relates to the stimulatory effect of the phosphoprotein, as wild-type Munc18c inhibits the ability of open Sx4 (and Sx4 lacking the N peptide) to form SNARE complexes (see Fig. S4). This is particularly important in light of a recent publication reporting stimulation of Sx4/SNAP23/VAMP2 complex-mediated liposome fusion by recombinant Munc18c produced in *Sf9* insect cells (35). It may be that Munc18c produced in *E. coli* (9) adopts a conformation analogous to that of wild-type Munc18c in adipocytes whereas that produced in insect cells is more similar to the phosphorylated protein.

This report provides the first demonstration of insulin-dependent changes in associations between members of the SNARE complex that regulates GLUT4 delivery to the cell surface. Our *in* vitro studies reveal inhibitory regulation of Sx4-containing SNARE complexes mediated by VAMP2 that can be lifted by phosphorylation of Munc18c. Our data are consistent with a model in which insulin regulates SNARE complex formation via a novel regulatory mechanism involving posttranslational modification of the SM protein. Given that SNAREs and SM proteins are central to all eukaryotic membrane trafficking events, this paves the way for identification of analogous mechanisms in other trafficking events that are regulated in response to external cues.

ACKNOWLEDGMENTS

We thank Bob White and Theo Kantidakis for help setting up the PLA, Frances Wason, Ewan Ramsay, Theo Laftsoglou, Luke Chamberlain, Lindsay Carpp, and Fiona Brandie for technical assistance and providing plasmids, and Chris MacDonald for critical reading of the manuscript.

This work was supported by a studentship from the BBRSC to D.K. and a project grant from Diabetes UK (11/0004289) to G.W.G. and N.J.B. N.J.B. is a Prize Fellow of the Lister Institute of Preventive Medicine.

REFERENCES

1. **Bryant NJ, Govers R, James DE.** 2002. Regulated transport of the glucose transporter GLUT4. Nat. Rev. Mol. Cell Biol. **3:**267–277. http://dx.doi.org/10.1038/nrm782.
2. **Bryant NJ, Gould GW.** 2011. SNARE proteins underpin insulin-regulated GLUT4 traffic. Traffic **12:**657–664. http://dx.doi.org/10.1111/j.1600-0854.2011.01163.x.
3. **Ungar D, Hughson FM.** 2003. Snare protein structure and function. Annu. Rev. Cell Dev. Biol. **19:**493–517. http://dx.doi.org/10.1146/annurev.cellbio.19.110701.155609.
4. **Aran V, Bryant NJ, Gould GW.** 2011. Tyrosine phosphorylation of Munc18c on residue 521 abrogates binding to Syntaxin 4. BMC Biochem. **12:**19. http://dx.doi.org/10.1186/1471-2091-12-19.
5. **Jewell JL, Oh E, Ramalingam L, Kalwat MA, Tagliabracci VS, Tackett L, Elmendorf JS, Thurmond DC.** 2011. Munc18c phosphorylation by the insulin receptor links cell signaling directly to SNARE exocytosis. J. Cell Biol. **193:**185–199. http://dx.doi.org/10.1083/jcb.201007176.
6. **Schmelzle K, Kane S, Gridley S, Lienhard GE, White FM.** 2006. Temporal dynamics of tyrosine phosphorylation in insulin signaling. Diabetes **55:**2171–2179. http://dx.doi.org/10.2337/db06-0148.
7. **Aran V, Brandie FM, Boyd AR, Kantidakis T, Rideout EJ, Kelly SM, Gould GW, Bryant NJ.** 2009. Characterisation of two distinct binding modes between Syntaxin 4 and Munc18c. Biochem. J. **419:**655–660. http://dx.doi.org/10.1042/BJ20082293.
8. **Rea S, Martin LB, McIntosh S, Macaulay SL, Ramsdale T, Baldini G, James DE.** 1998. Syndet, an adipocyte target SNARE involved in the insulin-induced translocation of GLUT4 to the cell surface. J. Biol. Chem. **273:**18784–18792. http://dx.doi.org/10.1074/jbc.273.30.18784.
9. **Brandie FM, Aran V, Verma A, McNew JA, Bryant NJ, Gould GW.** 2008. Negative regulation of syntaxin4/SNAP-23/VAMP2-mediated membrane fusion by Munc18c in vitro. PLoS One **3:**e4074. http://dx.doi.org/10.1371/journal.pone.0004074.
10. **Carpp LN, Ciufo LF, Shanks SG, BYoyd A, Bryant NJ.** 2006. The Sec1p/Munc18 protein Vps45p binds its cognate SNARE proteins via two distinct modes. J. Cell Biol. **173:**927–936. http://dx.doi.org/10.1083/jcb.200512024.
11. **Allalou A, Wahlby C.** 2009. BlobFinder, a tool for fluorescence microscopy image cytometry. Comput. Methods Programs Biomed. **94:**58–65. http://dx.doi.org/10.1016/j.cmpb.2008.08.006.
12. **Fredriksson S, Gullberg M, Jarvius J, Olsson C, Pietras K, Gustafsdottir SM, Ostman A, Landegren U.** 2002. Protein detection using proximity-dependent DNA ligation assays. Nat. Biotechnol. **20:**473–477. http://dx.doi.org/10.1038/nbt0502-473.
13. **Söderberg O, Gullberg M, Jarvius M, Ridderstråle K, Leuchowius KJ, Jarvius J, Wester K, Hydbring P, Bahram F, Larsson LG, Landegren U.** 2006. Direct observation of individual endogenous protein complexes in situ by proximity ligation. Nat. Methods **3:**995–1000. http://dx.doi.org/10.1038/nmeth947.
14. **Weibrecht I, Leuchowius KJ, Clausson CM, Conze T, Jarvius M, Howell WM, Kamali-Moghaddam M, Soderberg O.** 2010. Proximity ligation assays: a recent addition to the proteomics toolbox. Expert Rev. Proteomics **7:**401–409. http://dx.doi.org/10.1586/epr.10.10.
15. **Sutton RB, Fasshauer D, Jahn R, Brunger AT.** 1998. Crystal structure of a SNARE complex involved in synaptic exocytosis at 2.4 A resolution. Nature **395:**347–353. http://dx.doi.org/10.1038/26412.
16. **Hickson GR, Chamberlain LH, Maier VH, Gould GW.** 2000. Quantification of SNARE protein levels in 3T3-L1 adipocytes: implications for insulin-stimulated glucose transport. Biochem. Biophys. Res. Commun. **270:**841–845. http://dx.doi.org/10.1006/bbrc.2000.2525.
17. **Chamberlain LH, Gould GW.** 2002. The vesicle- and target-SNARE proteins that mediate Glut4 vesicle fusion are localized in detergent-insoluble lipid rafts present on distinct intracellular membranes. J. Biol. Chem. **277:**49750–49754. http://dx.doi.org/10.1074/jbc.M206936200.
18. **St-Denis JF, Cabaniols JP, Cushman SW, Roche PA.** 1999. SNAP-23 participates in SNARE complex assembly in rat adipose cells. Biochem. J. **338:**709–715. http://dx.doi.org/10.1042/0264-6021:3380709.
19. **Volchuk A, Wang Q, Ewart HS, Liu Z, He L, Bennett MK, Klip A.** 1996.

Syntaxin 4 in 3T3-L1 adipocytes: regulation by insulin and participation in insulin-dependent glucose transport. Mol. Biol. Cell **7:**1075–1082. http://dx.doi.org/10.1091/mbc.7.7.1075.

20. **Latham CF, Lopez JA, Hu SH, Gee CL, Westbury E, Blair DH, Armishaw CJ, Alewood PF, Bryant NJ, James DE, Martin JL.** 2006. Molecular dissection of the munc18c/syntaxin4 interaction: implications for regulation of membrane trafficking. Traffic **7:**1408–1419. http://dx.doi.org/10.1111/j.1600-0854.2006.00474.x.
21. **Calakos N, Bennett MK, Peterson KE, Scheller RH.** 1994. Protein-protein interactions contributing to the specificity of intracellular vesicular trafficking. Science **263:**1146–1149. http://dx.doi.org/10.1126/science.8108733.
22. **Hazzard J, Sudhof TC, Rizo J.** 1999. NMR analysis of the structure of synaptobrevin and of its interaction with syntaxin. J. Biomol. NMR **14:**203–207. http://dx.doi.org/10.1023/A:1008382027065.
23. **Liu W, Montana V, Bai J, Chapman ER, Mohideen U, Parpura V.** 2006. Single molecule mechanical probing of the SNARE protein interactions. Biophys. J. **91:**744–758. http://dx.doi.org/10.1529/biophysj.105.073312.
24. **Lang T, Jahn R.** 2008. Core proteins of the secretory machinery. Handb. Exp. Pharmacol. **2008:**107–127. http://dx.doi.org/10.1007/978-3-540-74805-2_5.
25. **Dulubova I, Sugita S, Hill S, Hosaka M, Fernandez I, Südhof TC, Rizo J.** 1999. A conformational switch in syntaxin during exocytosis: role of munc18. EMBO J. **18:**4372–4382. http://dx.doi.org/10.1093/emboj/18.16.4372.
26. **Nicholson KL, Munson M, Miller RB, Filip TJ, Fairman R, Hughson FM.** 1998. Regulation of SNARE complex assembly by an N-terminal domain of the t-SNARE Sso1p. Nat. Struct. Biol. **5:**793–802. http://dx.doi.org/10.1038/1834.
27. **Parlati F, Weber T, McNew JA, Westermann B, Sollner TH, Rothman JE.** 1999. Rapid and efficient fusion of phospholipid vesicles by the alpha-helical core of a SNARE complex in the absence of an N-terminal regulatory domain. Proc. Natl. Acad. Sci. U. S. A. **96:**12565–12570. http://dx.doi.org/10.1073/pnas.96.22.12565.
28. **Flaumenhaft R, Croce K, Chen E, Furie B, Furie BC.** 1999. Proteins of the exocytotic core complex mediate platelet alpha-granule secretion. Roles of vesicle-associated membrane protein, SNAP-23, and syntaxin 4. J. Biol. Chem. **274:**2492–2501.
29. **Scott BL, Van Komen JS, Irshad H, Liu S, Wilson KA, McNew JA.** 2004. Sec1p directly stimulates SNARE-mediated membrane fusion in vitro. J. Cell Biol. **167:**75–85. http://dx.doi.org/10.1083/jcb.200405018.
30. **Shen J, Tareste DC, Paumet F, Rothman JE, Melia TJ.** 2007. Selective activation of cognate SNAREpins by Sec1/Munc18 proteins. Cell **128:**183–195. http://dx.doi.org/10.1016/j.cell.2006.12.016.
31. **Stenkula KG, Lizunov VA, Cushman SW, Zimmerberg J.** 2010. Insulin controls the spatial distribution of GLUT4 on the cell surface through regulation of its postfusion dispersal. Cell Metab. **12:**250–259. http://dx.doi.org/10.1016/j.cmet.2010.08.005.
32. **Hatakeyama H, Kanzaki M.** 2011. Molecular basis of insulin-responsive GLUT4 trafficking systems revealed by single molecule imaging. Traffic **12:**1805–1820. http://dx.doi.org/10.1111/j.1600-0854.2011.01279.x.
33. **Bai L, Wang Y, Fan J, Chen Y, Ji W, Qu A, Xu P, James DE, Xu T.** 2007. Dissecting multiple steps of GLUT4 trafficking and identifying the sites of insulin action. Cell Metab. **5:**47–57. http://dx.doi.org/10.1016/j.cmet.2006.11.013.
34. **Bryant NJ, James DE.** 2001. Vps45p stabilizes the syntaxin homologue Tlg2p and positively regulates SNARE complex formation. EMBO J. **20:**3380–3388. http://dx.doi.org/10.1093/emboj/20.13.3380.
35. **Yu H, Rathore SS, Lopez JA, Davis EM, James DE, Martin JL, Shen J.** 2013. Comparative studies of Munc18c and Munc18-1 reveal conserved and divergent mechanisms of Sec1/Munc18 proteins. Proc. Natl. Acad. Sci. U. S. A. **110:**E3271–E3280. http://dx.doi.org/10.1073/pnas.1311232110.